Published in final edited form as:
Cell. 2014 February 27; 156(5): 1002–1016. doi:10.1016/j.cell.2014.01.040.

Serpins Promote Cancer Cell Survival and Vascular Cooption in Brain Metastasis

Manuel Valiente[1], **Anna C. Obenauf**[1], **Xin Jin**[1], **Qing Chen**[1], **Xiang H.-F. Zhang**[1,8], **Derek J. Lee**[1], **Jamie E. Chaft**[2], **Mark G. Kris**[2], **Jason T. Huse**[3,4], **Edi Brogi**[5], and **Joan Massagué**[1,4,6,7]

[1]Cancer Biology and Genetics Program, Memorial Sloan-Kettering Cancer Center, New York, NY 10065, USA

[2]Department of Medicine, Memorial Sloan-Kettering Cancer Center, New York, NY 10065, USA

[3]Human Oncology and Pathogenesis Program, Memorial Sloan-Kettering Cancer Center, New York, NY 10065, USA

[4]Brain Tumor Center, Memorial Sloan-Kettering Cancer Center, New York, NY 10065, USA

[5]Department of Pathology, Memorial Sloan-Kettering Cancer Center, New York, NY 10065, USA

[6]Metastasis Research Center, Memorial Sloan-Kettering Cancer Center, New York, NY 10065, USA

[7]Howard Hughes Medical Institute, Chevy Chase, MD 21205, USA

Abstract

Brain metastasis is an ominous complication of cancer, yet most cancer cells that infiltrate the brain die of unknown causes. Here we identify plasmin from the reactive brain stroma as a defense against metastatic invasion, and plasminogen activator (PA) inhibitory serpins in cancer cells as a shield against this defense. Plasmin suppresses brain metastasis in two ways: by converting membrane-bound astrocytic FasL into a paracrine death signal for cancer cells, and by inactivating the axon pathfinding molecule L1CAM that metastatic cells express for spreading along brain capillaries and for metastatic outgrowth. Brain metastatic cells from lung cancer and breast cancer express high levels of anti-PA serpins, including neuroserpin and serpin B2, to prevent plasmin generation and its deleterious consequences. By protecting cancer cells from death signals and fostering vascular cooption, anti-PA serpins provide a unifying mechanism for the initiation of brain metastasis in lung and breast cancers.

Joan Massagué, PhD, Box 116, Memorial Sloan-Kettering Cancer Center, 1275 York Avenue, New York, NY 10065 USA, Phone: 646-888-2044 j-massague@ski.mskcc.org.
[8]Present address: Lester and Sue Smith Breast Center, Baylor College of Medicine, One Baylor Plaza, Houston, TX 77030, USA

INTRODUCTION

Metastasis is the main cause of death from cancer, but biologically metastasis is a rather inefficient process. Most cancer cells that leave a solid tumor perish, and much of this attrition happens as circulating cancer cells infiltrate distant organs (Chambers et al., 2002). Although mechanisms for early steps of tumor cell dispersion and for late stages of macrometastatic outgrowth are known (Valastyan and Weinberg, 2011; Vanharanta and Massague, 2013), what factors determine the survival and adaptation of disseminated cancer cells in vital organs remain obscure. Identifying these factors is particularly critical in the case of brain metastasis. Brain relapse is the most devastating complication of cancer, with acute neurologic distress and high mortality as typical traits (Gavrilovic and Posner, 2005). The incidence of brain metastasis is ten times higher than that of all primary brain tumors combined (Maher et al., 2009). Lung cancer and breast cancer are the top sources of brain metastasis, together accounting for nearly two thirds of total cases. However, it is in the brain that infiltrating cancer cells face a particularly high rate of attrition, as shown in experimental models (Kienast et al., 2010). Brain metastasis tends to be a late complication of cancer in the clinic (Feld et al., 1984; Karrison et al., 1999) and is rare in mice with genetically engineered tumors that readily metastasize to other organs (Francia et al., 2011; Winslow et al., 2011).

The severe attrition of metastatic cells in the brain and the late occurrence of brain metastasis in the clinic argue that circulating cancer cells face major hurdles in colonizing this organ. Cancer cells require specialized mechanisms to traverse the blood-brain barrier (BBB), and molecular mediators of this process were recently identified (Bos et al., 2009; Li et al., 2013). However, most cancer cells that pass the BBB die (Heyn et al., 2006; Kienast et al., 2010). Interestingly, cancer cells that succeed at infiltrating the brain present the striking feature of adhering to the surface of capillaries and growing as a furrow around the vessels, whereas those that fail to coopt the vasculature also fail to thrive (Carbonell et al., 2009; Kienast et al., 2010; Lorger and Felding-Habermann, 2010). What kills most cancer cells that pass through the BBB, and what enables the few survivors to coopt the vasculature are questions of biologic and clinical interest.

Seeking to define common mechanisms for metastatic colonization of the brain, we focused on a small set of genes whose expression is associated with brain metastatic phenotypes both in lung and in breast adenocarcinoma models. One of these genes, *SERPINI1*, encoding the PA inhibitor neuroserpin, is normally expressed mainly in the brain. The plasminogen activators, tPA and uPA, convert plasminogen into plasmin, an endopeptidase that mediates fibrinolysis in blood clot resolution and is also involved in the stromal response to brain injury (Benarroch, 2007; Sofroniew and Vinters, 2010). Reactive astrocytes are major sources of PAs in ischemia and neurodegenerative injury (Adhami et al., 2008; Ganesh and Chintala, 2011; Teesalu et al., 2001). To avert the deleterious action of plasmin neurons express neuroserpin (Yepes et al., 2000). We found that by secreting PA inhibitory serpins brain metastatic cells thwart the lethal action of plasmin from the reactive stroma. Moreover, suppression of Fas-mediated cancer cell killing and promotion of L1CAM-mediated vascular cooption lie downstream of anti-PA serpin action as critical requirements for the initiation of brain metastasis.

RESULTS

Association of PA-inhibitory serpins with the brain metastatic phenotype

To identify shared mediators of brain metastasis we compared transcriptomic signatures of brain metastatic subpopulations (BrM) that were isolated from lymph node-derived human lung adenocarcinoma cell lines H2030 and PC9 (Nguyen et al., 2009) and from pleural effusion-derived breast cancer cell lines MDA-MB-231 (MDA231 for short) and CN34 (Bos et al., 2009) (Figure 1A). Seven genes were upregulated in brain metastatic cells compared to the source parental lines in at least three of the four models (Figure S1A). Among these genes, *LEF1* was previously defined as a mediator of WNT signaling in brain metastasis (Nguyen et al., 2009). Of the remaining genes, only *SERPINI1*, encoding neuroserpin (NS), was associated with brain relapse in human primary tumors (see below). This was intriguing because NS expression is normally restricted to neurons, where it protects from PA cytotoxicity (Yepes et al., 2000).

The 36 serpin family members in human collectively target 18 proteases (Irving et al., 2000). Four serpins –NS and serpins B2, E1, and E2– selectively inhibit PA (Law et al., 2006). mRNA levels for three of the four were upregulated >3-fold in brain metastatic cells (Figure 1A). Only one other serpin, *SERPIND1*, was also upregulated (Figure 1A). Serpin D1 inhibits thrombin, which cooperates with plasminogen in cerebral injury (Fujimoto et al., 2008). Bone metastatic derivatives (MDA231-BoM) (Kang et al., 2003) and lung metastatic derivatives (MDA231-LM2) (Minn et al., 2005) were available for comparisons with MDA231-BrM2, and showed little or no upregulation of the serpins (Figure 1B).

Additionally, we established the cell line ErbB2-P from a mouse mammary tumor driven by a mutant *ErbB2* transgene (Muller et al., 1988) and then isolated a brain metastatic derivative (ErbB2-BrM2) by selection of ErbB2-P in congenic mice. ErbB2-BrM2 cells showed a strong upregulation of serpins B2 and D1 compared to ErbB2-P (Figure 1A). We also screened four cell lines derived from lymph node metastases of genetically engineered $Kras^{G12D};p53^{-/-}$ mouse lung adenocarcinomas (Winslow et al., 2011). All four lines were highly metastatic to visceral organs but ranged widely in brain metastatic activity (Figures 1C, S1B), and brain metastasis was associated with high expression of serpins I1, B2, E2 and/or D1 (Figure 1C,D).

The upregulation of NS and serpin B2 in brain metastatic cells was confirmed at the protein level (Figure S1C,D). Moreover, conditioned media from brain metastatic cells inhibited the generation of plasmin activity from plasminogen (Figures 1E,F and S1E). The only exception was PC9-BrM3, a cell line that is less aggressive in brain metastasis compared to H2030-BrM3 (Nguyen et al., 2009) and lacks upregulated anti-PA serpins (Figure 1A, S1C,D).

Neuroserpin and serpin B2 in human brain metastasis tissues

Focusing on the two most frequently upregulated anti-PA serpins in these models, NS and serpin B2, we queried gene-expression data from 106 primary lung adenocarcinomas with relapse annotation (Nguyen et al., 2009). The expression level of *SERPINI1* and *SERPINB2* in the tumors was associated with brain relapse, both as individual genes (data not shown)

and combined (p = 0.018, hazard ratio = 2.33 +/− 0.3; Figure 1G). Expression of the two genes was not significantly associated with metastasis to bone or lungs (p = 0.89, hazard ratio = 0.91 +/− 0.33; p = 0.36, hazard ratio = 0.76 +/− 0.27; Figure S1F,G). *SERPINI1* and *SERPINB2* expression in breast tumors was not a predictor of brain metastasis (p = 0.21, hazard ratio = 0.96 +/− 0.16; Figure S1H), though in most of these cases brain relapse was a late event that might have been seeded from metastases in other organs.

Immunohistochemical analysis of NS and serpin B2 in human brain metastasis tissue was done using as a reference mouse brain lesions formed by serpin-expressing human cancer cells (Figure S1I). Among 33 metastases of non-small cell lung carcinomas, 45% scored positive for NS and 94% for serpin B2. Among 123 from various subtypes of breast cancer, 77% scored positive for NS and 34% for serpin B2 (Figures 1H,I and S1I,J). The immunoreactivity was diffusely distributed in the cytoplasm of carcinoma cells and only minimally in the scant extracellular stroma. Positivity for NS and serpin B2 in the inflammatory infiltrate was limited.

Plasmin is lethal to cancer cells that invade the brain parenchyma

The MDA231-BrM2 or H2030-BrM3 models are metastatic to the brain from orthotopic tumors and from the arterial circulation (Bos et al., 2009; Nguyen et al., 2009). We inoculated these cells into the arterial circulation of immunodeficient mice via the left cardiac ventricle and fixed the tissue to count cancer cells lodged in the brain capillary network at different time points (Figures 2A–C, S2A). One day after inoculation, we observed isolated cancer cells trapped within brain capillaries (Figure 2B, and H2030-BrM3 data not shown). Cells passing through the BBB were observed between days 2 and 7 after inoculation (Figures 2B, S2B). All cells remaining within capillaries on day 7 stained positive for the apoptosis marker, cleaved caspase-3 (Figure S2C,D). No intravascular cells were observed thereafter. In parental MDA231 the number of extravasated cells dropped sharply after day 5 and rarely recovered (Figure S2B). In line with previous reports (Kienast et al., 2010; Lorger and Felding-Habermann, 2010), >90% of cancer cells entering the brain disappeared within days. In MDA231-BrM2 the number of extravasated cells increased until day 7, dropped sharply by day 10, but recovered by day 16. The survivors were bound to and stretched over the abluminal surface of brain capillaries (Figure 2A,B). Outgrowth mainly occurred on coopted vessels (Figure 2C, summarized in Figure 2D).

In the brain, metastatic cells were in close proximity to astrocytes (Figures 2E, S2E,F), microglia and neurons (Figure S2G–J). Reactive astrocytes, identified by high GFAP expression and a stellate morphology, were associated with cancer cells right after extravasation and thereafter (Figures 2E, S2E,F). Reactive astrocytes are a major source of PA in brain injury (Adhami et al., 2008; Ganesh and Chintala, 2011). Indeed, mouse brain sections harboring metastatic cells showed tPA and uPA immunoreactivity associated with astrocytes (Figures 2F,G). Mouse astrocytes cultures were superior to microglia at converting plasminogen to plasmin (Figure S2K). Neurons produce plasminogen for neurite and synapse formation (Gutierrez-Fernandez et al., 2009). Plasminogen immunoreactivity was associated with NeuN+ neurons near metastatic cells in mouse brain (Figure 2H). Thus,

the brain metastasis microenvironment contains the necessary components for plasmin production.

To determine whether plasmin is harmful to metastatic cells in the brain parenchyma we used mouse brain slice cultures (Figure 2I). When placed on top of brain slices H2030-BrM3 cells migrated into the tissue, targeted blood capillaries, and spread on the surface of the vessels (Figure 2J). H2030-BrM3 cells proliferated under these conditions (Figure 2K,L), whereas parental H2030 did not proliferate (Figure 2K,L) and underwent apoptosis (Figure 2M,N). Similar results were obtained with MDA231 cells (Figure S2N). In co-cultures of cancer cells with astrocytes and microglia, plasminogen addition triggered apoptosis in parental H2030 but not in H2030-BrM3 (Figure S2L,M). The brain slices contained endogenous plasmin activity, and addition of a plasmin inhibitor, α2-antiplasmin (Bajou et al., 2008), inhibited this activity (Figure S2O,P) and increased the survival of parental H2030 cells in the slices (Figure 2K–N). Of note, addition of plasmin to cancer cell monolayer cultures did not trigger apoptosis (Figure S2Q). These results suggested that plasmin acting through unknown substrates kills infiltrating cancer cells in the brain, whereas highly metastatic cells are shielded from this threat (Figure 2O).

Neuroserpin protects metastatic cells from plasmin-mediated attrition

To investigate the role of NS in brain metastasis we first used the H2030-BrM3 model, in which only this serpin is upregulated (refer to Figure 1A). Brain lesions formed by H2030-BrM3 cells showed strong NS immunoreactivity (Figure S3A). Two shRNAs that decreased NS expression and secretion by >85% (Figure S3B,C) did not affect the growth of H2030-BrM3 cells in culture (Figure S3D) but inhibited the metastatic activity of these cells, as shown by bioluminescence imaging (BLI) of marker luciferase in-vivo (Figure 3A–D), BLI ex-vivo (Figures 3B), and marker green fluorescent protein (GFP) expression in brain sections (Figure 3E). NS depletion in H2030-BrM3 decreased the number and size of brain lesions (Figures 3F, S3E), with a >90% overall reduction in brain tumor burden (Figure 3G). The few macroscopic lesions that developed were rich in NS (Figure S3F), suggesting escape from the knockdown.

NS knockdown did not inhibit the entry of H2030-BrM3 cells into the brain parenchyma (Figure S3G) or their ability to cross an endothelial/astrocyte BBB-like barrier in vitro, whereas the knockdown of *ST6GalNaC5*, a mediator of BBB extravasation, did (Bos et al., 2009) (Figure S3H,I). In brain slice assays, NS knockdown in H2030-BrM3 cells decreased the number of infiltrated cells (Figure 3H,I) and increased apoptosis (Figure 3H,J), whereas overexpression of NS in parental H2030 and MDA231 cells had the opposite effects (Figure 3K,L).

Brain metastasis mediated by the PA inhibitory function of neuroserpin

PC9-BrM3 can infiltrate the brain but are less aggressive than H2030-BrM3 at colonizing it (Nguyen et al., 2009) and show no upregulation of anti-PA serpins (refer to Figure 1A). PC9-BrM3 cells were stably transduced with vectors encoding the wild type NS or a mutant (NSΔloop) that is devoid of PA inhibitory function (Takehara et al., 2009) (Figure S3J–M). Wild type NS significantly increased the brain metastatic activity of PC9-BrM3 whereas the

mutant did not (Figure 3M,N). PC9-BrM3 cells are also metastatic to bone (Nguyen et al., 2009); NS overexpression did not markedly affect this activity (Figure 3M,N). $NS^{\Delta loop}$ was also ineffective at protecting the parental H2030 and MDA231 cells from apoptosis in brain tissue (Figure 3K,L). These results suggest that NS mediates brain metastatic activity in cancer cells by inhibiting PA.

Role of anti-PA serpins in brain metastatic breast cancer cells

Unlike the H2030-BrM3 cells, most other brain metastatic models and a large proportion of human brain metastatic tissues overexpressed not one but multiple anti-PA serpins (refer to Figure 1A,I). In MDA231-BrM2, a triple knockdown of the three overexpressed serpins – serpins B2, D1 and NS– (Figure S4A–C) inhibited the brain metastatic activity of the cells more than did the knockdown of any individual serpin (Figures 4A,B, S4G,H). The knockdown of serpin B2 (Figure S4D,E) partially inhibited the brain metastatic activity of MDA231-BrM2, and the lost activity could be rescued by enforced overexpression of NS (Figures 4A,B, S4F). Clonal cell lines isolated from the MDA231-BrM2 population showed heterogeneity in the overexpression of anti-PA serpins. Compared to the parental MDA231 population, NS was upregulated in 9/10 of the clones, serpin B2 in 5/10 and serpin D1 in 8/10 (Figures 4C, S4I). As a trend, clones with high levels of the three serpins were more metastatic to brain than were clones overexpressing fewer (Figures 4D, S4J). Clones with high levels of NS and serpin D1 lost brain metastatic activity when transduced with *NS* shRNA (Figure 4E). In the ErbB2- BrM2 model the knockdown of its only overexpressed anti-PA serpin, serpin B2 (refer to Figure 1A), strongly decreased the brain metastatic activity in immunocompetent mice (Figure 4F–H). In sum, the evidence indicated that expression of one or more anti-PA serpins provides lung cancer and breast cancer cells with a critical advantage in the formation of brain metastases.

Metastatic cells face FasL in the brain

We searched plasmin substrate databases (MEROPS, CutDB) for proteins whose cleavage might affect brain metastasis (Bajou et al., 2008; Chen and Strickland, 1997; Nayeem et al., 1999; Pang et al., 2004). We focused first on FasL, a pro-apoptotic cytokine. FasL is a membrane-anchored homotrimeric protein that binds to Fas, a receptor that activates pro-apoptotic caspases through the adaptor protein FADD (Ashkenazi and Dixit, 1998). FasL is highly expressed in reactive astrocytes in ischemia, brain trauma, Alzheimer's disease, encephalomyelitis and multiple sclerosis (Choi and Benveniste, 2004). Astrocytes are the main source of FasL against invading T cells in encephalomyelitis (Wang et al., 2013). Plasmin cleaves FasL at Arg144, releasing sFasL as a diffusible cell death signal (Bajou et al., 2008; Fang et al., 2012). Therefore, we asked whether anti-PA serpins shield cancer cells from the lethal action of plasmin-mobilized sFasL (Figure 5A).

FasL immunoreactivity in brain sections harboring H2030-BrM3 lesions was concentrated on reactive astrocytes (Figures 5B, S5A). Human and mouse astrocytes expressed FasL in culture (Figures 5C, S5B). Addition of plasminogen decreased the level of cell-bound FasL in these cultures and increased sFasL in the supernatants (Figures 5C,D, S5C–E). Addition of anti-PA serpins or antiplasmin decreased the level of sFasL in mouse brain slices (Figure

5E). These results showed that the PA-plasmin system can mobilize stromal FasL in response to metastatic invasion of the brain.

H2030, PC9, MDA231 and CN34 expressed Fas, as did their BrM derivatives (Figure S5F). Addition of sFasL caused apoptosis in BrM cells in monolayer cultures (Figure S5G–I) and in brain tissue (Figure 5F–H), even in the presence of α2-antiplasmin (Figure S5J). Conversely, addition of anti-FasL blocking antibody protected parental H2030 cells from apoptosis in brain tissue (Figure 5G–I). Thus, brain metastatic cells are susceptible to apoptosis if exposed to sFasL in the brain parenchyma, and this occurs downstream of plasmin.

Neuroserpin shields brain metastatic cells from Fas-mediated killing

To determine whether Fas signaling caused the death of cancer cells that infiltrated the brain, we used a FADD truncation mutant that lacks the death effector domain (FADD-DD construct) and acts as a dominant-negative inhibitor of Fas signaling (Chinnaiyan et al., 1996) (Figure 5J). Transduction of FADD-DD in H2030-BrM3 cell line (Figure 5K) prevented the activation of caspase 3 by sFasL (Figure 5L). The apoptosis that anti-PA serpin-depleted BrM cells suffer in brain tissue (refer to Figures 3H–J, S5L) could be prevented by adding anti-FasL blocking antibodies to the tissue cultures as well as by enforcing the expression of FADD-DD in the cancer cells (Figures 5M,N, S5L). Moreover, FADD-DD partially rescued the metastatic activity of NS-depleted H2030-BrM3 (Figure 5O). Collectively, these results showed that anti-PA serpin activity shields metastatic cells from FasL attack in the brain.

The plasmin target L1CAM mediates cancer cell adhesion

Although inhibition of Fas signaling with FADD-DD protected NS-depleted cancer cells from death in the brain it did not fully restore their metastatic activity (Figure 5O). The NS-depleted, FADD-DD expressing H2030-BrM3 cells formed smaller lesions that were less well organized (Figure S6A). Therefore we postulated that anti-PA serpins promote brain metastasis by doing more than just preventing FasL action.

Several clues led us to consider L1 cell adhesion molecule (L1CAM) as relevant mediator of metastasis in this context. L1CAM is mainly expressed in neural tissues and in tumors (Schafer and Altevogt, 2010). It consists of six immunoglobulin-like (Ig) domains, five fibronectin-like (FN) domains, a transmembrane region, and an intracellular domain (Figure 6A). The L1CAM Ig-like repeats mediate homo- and heterophilic interactions for axon guidance (Maness and Schachner, 2007). L1CAM binds to itself, to integrins (Felding-Habermann et al., 1997) and to other proteins (Castellani et al., 2002; Donier et al., 2012; Kulahin et al., 2008). L1CAM expression in tumors is implicated in invasion (Voura et al., 2001) and associated with poor prognosis (Doberstein et al., 2011; Schroder et al., 2009). Plasmin cleaves L1CAM at dibasic motifs (Lys860/Lys863), disrupting the capacity for cell adhesion (Nayeem et al., 1999; Silletti et al., 2000) (Figure 6A).

Hence, we postulated that L1CAM mediates plasmin-sensitive vascular cooption by metastatic cells in the brain. L1CAM was expressed in the cancer cell lines regardless of their metastatic activity, tumor type, or species of origin (Figure S6B,C). H2030-BrM3 cells

readily adhered to monolayers of human brain microvascular endothelial cells (HBMEC) (Figure 6B,C) and to monolayers of their own (Figure 6D). RNAi-mediated knockdown of L1CAM (Figure S6B) inhibited these cell-cell binding activities (Figure 6C,D). Addition of plasmin to cancer cell monolayers caused a decrease in cellassociated L1CAM levels, as shown by flow cytometry (Figure 6E) and by the accumulation of a 150kDa fragment in the media (Figure 6F) (Mechtersheimer et al., 2001). Moreover, plasmin-treated H2030-BrM3 cells lost cell adhesion capacity (Figure 6G,H).

L1CAM mediates vascular co-option and metastatic outgrowth

The molecular basis for vascular cooption in cancer remains unknown. We determined whether L1CAM participates in vascular cooption by metastatic cells in the brain. L1CAM-depletion in H2030-BrM3 cells did not affect their ability to grow in culture (Figure S6D), infiltrate brain tissue, or seek capillaries (Figures 6I, S6E). Notably, L1CAM depletion significantly reduced the ability of H2030-BrM3 and MDA231-BrM2 cells to spread on the abluminal surface of the capillaries (Figures 6I,J, S6G). This was accompanied with a marked decrease in the proliferation marker Ki67 in vessel-associated cancer cells (Figure 6K), without changes in apoptosis markers (Figure S6F).

PC9-BrM3 cells, which do not overexpress endogenous anti-PA serpins, had a limited ability to spread on brain capillaries (Figure 6L,M). Enforced expression of NS in these cells not only augmented their metastatic activity (see Figure 3N) but it also increased their spreading on brain capillaries (Figure 6L,M) and their proliferation on the coopted vessels (Figure 6N). L1CAM depletion in PC9-BrM3-NS cells (Figure S6H,I) abrogated these NS-dependent gains (Figure 6L–N).

L1CAM supports metastasis initiation downstream of neuroserpin

L1CAM immunostaining was clearly detectable on carcinoma cells in a majority of human NSCLC brain metastasis samples examined, and tended to be concentrated at cell interfaces (Figure S7A,B). L1CAM-positive cells were present in clusters. In the brain of inoculated mice, extravasated H2030-BrM3 cells were spread over the basal lamina of capillaries, without discernable contacts with the endothelial cells (Figure 7A). L1CAM immunostaining in micrometastases was concentrated at the interfaces of cancer cells with capillaries and with adjacent cancer cells (Figure 7B). In recently extravasated H2030-BrM3 cells L1CAM-depletion allowed cell contact with capillaries but prevented cell spreading over the capillaries (Figure 7C). Twenty-one days later, L1CAM-depleted cells remained mostly as single cells or small clusters whereas the wild type cells readily expanded over the capillary network and formed large colonies (Figure 7D,E). L1CAM knockdown markedly decreased the overall brain metastatic activity of H2030-BrM3 and MDA231-BrM2 cells (Figure 7F–H). Moreover, L1CAM depletion abrogated the gain in metastatic activity of PC9-BrM3 cells imparted by enforced NS overexpression (Figure 7I). These results argued that L1CAM expression in metastatic cells acts downstream of NS to mediate cooption of brain capillaries and metastatic outgrowth.

DISCUSSION

The growing incidence of brain metastasis warrants a better understanding of the molecular mechanisms that underlie this condition. Our findings illuminate two critical requisites for metastatic colonization of the brain, namely, the escape of infiltrating cancer cells from killing by reactive stromal signals, and the striking ability of the surviving cancer cells to coopt brain capillaries for metastatic expansion. We show that a stromal PA-plasmin pathway and its inhibition by carcinoma serpins control both of these processes in brain metastasis from lung and breast cancers, suggesting a unified mechanism for metastatic colonization of the brain.

Anti-PA serpins as common mediators of brain metastasis

Brain metastasis involves close and sustained interactions of cancer cells with brain capillaries and reactive astrocytes. Previous work (Carbonell et al., 2009; Kienast et al., 2010; Lorger and Felding-Habermann, 2010) and our own show that circulating cancer cells interact with capillary walls not only during extravasation but also thereafter, by attaching to the abluminal surface and growing as a furrow along the coopted vessels. Cancer cells that infiltrate the brain are immediately exposed to astrocytes that abound in the perivascular space and produce deleterious signals to repel invading cells. Cancer cells must be shielded from such signals in order to survive and to extract benefits from the stroma, including benefits from astrocytes (Lin, 2010; Seike et al., 2011). We show that the expression of anti-PA serpins in cancer cells provides such a shield. Three out of four known anti-PA serpins, and serpin D1 are expressed in our six brain metastasis models. The most prominent of these serpins, NS and B2, are expressed in a majority of brain metastases from lung cancer and breast cancer patients. The PA-plasmin system is well characterized in connection with its role in blood clot resolution, but its role in cancer has remained paradoxical. Although plasmin can promote cancer cell proliferation and invasion by cleaving growth factor precursors and extracellular matrix proteins (McMahon and Kwaan, 2008), anti-PA serpin levels in tumors and in blood are associated with poor outcome in many cancers (Berger, 2002; Foekens et al., 1995; Harbeck et al., 1999). Here we show that anti-PA serpins shield metastatic cells from PA-plasmin in the brain, providing a clear pro-metastatic advantage.

Averting Fas killing and protecting L1CAM vascular cooption

Although FasL plays important roles in immune homeostasis (Krammer, 2000) and is present in tumors (Baldini et al., 2009) its expression is particularly acute in reactive astrocytes (Beer et al., 2000). Astrocytes are the main source of FasL in response to infiltrating leukocytes, and of PAs in response to brain injury. We show that metastasis-associated astrocytes express both PA and FasL. Plasmin releases membrane-bound FasL from astrocytes, and sFasL levels in brain tissue depend on plasmin. Brain metastatic cells from lung or breast cancers suffer Fas-dependent death in the brain unless they are protected by anti-PA serpins. We conclude that Fas signaling mediates, and anti-PA serpins prevent the attrition of infiltrating cancer cells in the brain.

We show that L1CAM mediates metastatic cells spread on the vasculature and it additionally mediates interactions between cancer cells. If depleted of L1CAM, cancer cells

fail to coopt brain capillaries, and metastatic outgrowth stalls. Cancer cell-derived anti-PA serpins prevent plasmin destruction of L1CAM, providing yet another benefit besides averting Fas-mediated cancer cell killing. L1CAM expression is normally restricted to neurons where it mediates axonal guidance through highly plastic interactions of the growth cone with surrounding components (Wiencken-Barger et al., 2004). The dynamic nature of L1CAM adhesive interactions might be particularly advantageous to cancer cells in their quest to coop vasculature while invading tissue. Although the molecular basis for vascular cooption in cancer is largely unknown, the present identification of L1CAM as a mediator provides an opening for the mechanistic dissection of this process.

Implications beyond brain metastasis

The molecular mechanisms defined here protect metastatic cells from selective pressures that are particularly acute in the brain. However, a high mortality of infiltrating cancer cells is characteristic of metastasis in general (Gupta and Massagué, 2006; Valastyan and Weinberg, 2011), and vascular cooption occurs in metastasis to other organs and by other types of cancer (Donnem et al., 2013). Vascular cooption also provides cancer cells with an escape from therapy-induced hypoxia (Leenders et al., 2004). The anti-PA serpins that are up-regulated in our brain metastatic models are also expressed, albeit at lower levels, in counterparts metastatic to other organs. Moreover, L1CAM expression in primary tumors is associated with poor prognosis in various types of cancer, as are PA, plasmin, and FasL. The reactive brain stroma, with its high capacity to generate PA-plasmin and FasL, may be more challenging to infiltrating cancer cells than is the stroma in other organs and, as a result, it may select for accentuated versions of otherwise general metastatic traits. Although anti-PA serpins, plasmin, FasL and L1CAM had not been previously connected to metastatic cell survival and vascular cooption, their repeated clinical association with poor prognosis and the mechanistic links exposed in the present work may reflect a wider role in cancer than is shown here.

EXPERIMENTAL PROCEDURES

Animal studies

All animal experiments were done in accordance to a protocol approved by MSKCC Institutional Animal Care and Use Committee (IACUC). Athymic NCR nu/nu, Cr:NIH bg-nu-xid, FVB/NCr (all from NCI-Frederick), and B6129SF1/J (Jackson Lab) female mice aged between 4–6 weeks were used. Brain metastatic derivatives of a syngeneic ErbB2 model (ErbB2-BrM2) were established following the previous protocol (Bos et al., 2009; Nguyen et al., 2009) and is detailed in EXTENDED EXPERIMENTAL PROCEDURES. Brain colonization assays were performed as follows: 50,000 (for long term experiments) or 500,000 (for short term experiments) of MDA231-BrM2a, CN34BrM-2c, H2030-BrM3, PC9-BrM3 and 100,000 for syngeneic cell lines 373N1, 393N1, 482N1, 2691N1, ErbB2-BrM2 cells in 100μl of PBS were injected in the left ventricle. Brain colonization was analyzed in-vivo and ex-vivo by bioluminescence imaging (BLI). Anesthetized mice (ketamine 100mg/kg/xylazine 10mg/kg) were injected retro-orbitally with D-Luciferin (150mg/kg) and imaged with an IVIS Spectrum Xenogen machine (Caliper Life Sciences). Bioluminescence analysis was performed using Living Image software, version 2.50.

Brain slice assays

Organotypic slice cultures from adult mouse brain were prepared adapting previously described methods (Polleux and Ghosh, 2002). Brains (4–6 week old athymic NCR nu/nu mice) were dissected in Hank's Balanced Salt Solution (HBSS) supplemented with HEPES (pH 7.4) (2.5mM), D-glucose (30mM), $CaCl_2$ (1mM), $MgSO_4$ (1mM), $NaHCO_3$ (4mM), and were embedded in low-melting agarose (Lonza) pre-heated at 42° C. The embedded brains cut into 250μm slices using a vibratome (Leica). Brain slices (bregma −1mm to +3mm) were placed with flat spatulas on top of 0.8μm pore membranes (Millipore) in slice culture media (DMEM, supplemented HBSS, FBS 5%, LGlutamine (1mM), 100IU/mL penicillin, 100μg/mL streptomycin). Brain slices were incubated at 37°C and 5% CO_2 for 1 h, and then 3×10^4 cancer cells suspended in 2 μL of culture media were placed on the surface of the slice and incubated for 48–72 hours. Brain slices could be maintained under these conditions for up to five days without apparent alterations in tissue architecture. α2-antiplasmin (Molecular Innovations, 2.5μg/ml), NS and serpin B2 (Peprotech, 0.5μg/ml each) were added to the medium. sFasL (Peprotech, 500ng/ml) or FasL blocking antibodies (BD, 12.5μg/ml) were added to the medium, and slices pre-incubated for 24 hours before addition of cancer cells. Brain slices were fixed in PFA 4%, overnight and then free-floating immunofluorescence performed for GFP (Aves lab, ref. GFP-1020, 1:1000), cleaved caspase-3 (Cell Signaling, ref. 9661, 1:500), collagen IV (Millipore, ref. AB756P, 1:500). Nuclei were stained with Bis-Benzamide (SIGMA, 1μg/ml). Slices were mounted with ProLong Gold anti fade reagent (Invitrogen).

Supplementary Material

Refer to Web version on PubMed Central for supplementary material.

Acknowledgments

We thank A. Boire, P. Bos, L. DeAngelis, E. Holland and J. Posner for helpful input, the Brain Tumor Center for tumor samples, Marija Drobnjak for establishing tissue microarray from lung cancer brain metastasis, T. Jacks for cell lines and A. Thorburn for reagents. This work was supported by NIH grants P01-CA129243 and U54-163167, DOD Innovator award W81XWH-12-0074, and the Alan and Sandra Gerry Metastasis Research Initiative (J.M.). M.V. is a Hope Funds for Cancer Research postdoctoral fellow. A.C.O. is an Erwin Schrödinger Fellowship awardee (J3013, FWF, Austrian Science Fund). X.Z. is a McNair Scholar and the recipient of a grant from Breast Cancer Research Foundation. J.M. is an investigator of the Howard Hughes Medical Institute.

REFERENCES

Adhami F, Yu D, Yin W, Schloemer A, Burns KA, Liao G, Degen JL, Chen J, Kuan CY. Deleterious effects of plasminogen activators in neonatal cerebral hypoxia-ischemia. Am J Pathol. 2008; 172:1704–1716. [PubMed: 18467699]

Ashkenazi A, Dixit VM. Death receptors: signaling and modulation. Science. 1998; 281:1305–1308. [PubMed: 9721089]

Bajou K, Peng H, Laug WE, Maillard C, Noel A, Foidart JM, Martial JA, DeClerck YA. Plasminogen activator inhibitor-1 protects endothelial cells from FasL-mediated apoptosis. Cancer Cell. 2008; 14:324–334. [PubMed: 18835034]

Baldini E, Ulisse S, Marchioni E, Di Benedetto A, Giovannetti G, Petrangeli E, Sentinelli S, Donnorso RP, Reale MG, Mottolese M, et al. Expression of Fas and Fas ligand in human testicular germ cell tumours. Int J Androl. 2009; 32:123–130. [PubMed: 17916181]

Beer R, Franz G, Schopf M, Reindl M, Zelger B, Schmutzhard E, Poewe W, Kampfl A. Expression of Fas and Fas ligand after experimental traumatic brain injury in the rat. J Cereb Blood Flow Metab. 2000; 20:669–677. [PubMed: 10779011]

Benarroch EE. Tissue plasminogen activator: beyond thrombolysis. Neurology. 2007; 69:799–802. [PubMed: 17709713]

Berger DH. Plasmin/plasminogen system in colorectal cancer. World J Surg. 2002; 26:767–771. [PubMed: 11965442]

Bos PD, Zhang XH, Nadal C, Shu W, Gomis RR, Nguyen DX, Minn AJ, van de Vijver MJ, Gerald WL, Foekens JA, et al. Genes that mediate breast cancer metastasis to the brain. Nature. 2009; 459:1005–1009. [PubMed: 19421193]

Carbonell WS, Ansorge O, Sibson N, Muschel R. The vascular basement membrane as "soil" in brain metastasis. PloS one. 2009; 4:e5857. [PubMed: 19516901]

Castellani V, De Angelis E, Kenwrick S, Rougon G. Cis and trans interactions of L1 with neuropilin-1 control axonal responses to semaphorin 3A. EMBO J. 2002; 21:6348–6357. [PubMed: 12456642]

Chambers AF, Groom AC, MacDonald IC. Dissemination and growth of cancer cells in metastatic sites. Nat Rev Cancer. 2002; 2:563–572. [PubMed: 12154349]

Chen ZL, Strickland S. Neuronal death in the hippocampus is promoted by plasmin-catalyzed degradation of laminin. Cell. 1997; 91:917–925. [PubMed: 9428515]

Chinnaiyan AM, Tepper CG, Seldin MF, O'Rourke K, Kischkel FC, Hellbardt S, Krammer PH, Peter ME, Dixit VM. FADD/MORT1 is a common mediator of CD95 (Fas/APO-1) and tumor necrosis factor receptor-induced apoptosis. J Biol Chem. 1996; 271:4961–4965. [PubMed: 8617770]

Choi C, Benveniste EN. Fas ligand/Fas system in the brain: regulator of immune and apoptotic responses. Brain Res Rev. 2004; 44:65–81. [PubMed: 14739003]

Doberstein K, Wieland A, Lee SB, Blaheta RA, Wedel S, Moch H, Schraml P, Pfeilschifter J, Kristiansen G, Gutwein P. L1-CAM expression in ccRCC correlates with shorter patients survival times and confers chemoresistance in renal cell carcinoma cells. Carcinogenesis. 2011; 32:262–270. [PubMed: 21097529]

Donier E, Gomez-Sanchez JA, Grijota-Martinez C, Lakoma J, Baars S, Garcia-Alonso L, Cabedo H. L1CAM binds ErbB receptors through Ig-like domains coupling cell adhesion and neuregulin signalling. PloS one. 2012; 7:e40674. [PubMed: 22815787]

Donnem T, Hu J, Ferguson M, Adighibe O, Snell, Harris AL, Gatter KC, Pezzella F. Vessel co-option in primary human tumors and metastases: an obstacle to effective anti-angiogenic treatment? Cancer Med. 2013; 2:427–436. [PubMed: 24156015]

Fang H, Placencio VR, DeClerck YA. Protumorigenic activity of plasminogen activator inhibitor-1 through an antiapoptotic function. J Natl Cancer Inst. 2012; 104:1470–1484. [PubMed: 22984202]

Feld R, Rubinstein LV, Weisenberger TH. Sites of recurrence in resected stage I non-small-cell lung cancer: a guide for future studies. J Clin Oncol. 1984; 2:1352–1358. [PubMed: 6512581]

Felding-Habermann B, Silletti S, Mei F, Siu CH, Yip PM, Brooks PC, Cheresh DA, O'Toole TE, Ginsberg MH, Montgomery AM. A single immunoglobulin-like domain of the human neural cell adhesion molecule L1 supports adhesion by multiple vascular and platelet integrins. J Cell Biol. 1997; 139:1567–1581. [PubMed: 9396761]

Foekens JA, Look MP, Peters HA, van Putten WL, Portengen H, Klijn JG. Urokinase-type plasminogen activator and its inhibitor PAI-1: predictors of poor response to tamoxifen therapy in recurrent breast cancer. J Natl Cancer Inst. 1995; 87:751–756. [PubMed: 7563153]

Francia G, Cruz-Munoz W, Man S, Xu P, Kerbel RS. Mouse models of advanced spontaneous metastasis for experimental therapeutics. Nat Rev Cancer. 2011; 11:135–141. [PubMed: 21258397]

Fujimoto S, Katsuki H, Ohnishi M, Takagi M, Kume T, Akaike A. Plasminogen potentiates thrombin cytotoxicity and contributes to pathology of intracerebral hemorrhage in rats. J Cereb Blood Flow Metab. 2008; 28:506–515. [PubMed: 17940541]

Ganesh BS, Chintala SK. Inhibition of reactive gliosis attenuates excitotoxicity-mediated death of retinal ganglion cells. PloS one. 2011; 6:e18305. [PubMed: 21483783]

Gavrilovic IT, Posner JB. Brain metastases: epidemiology and pathophysiology. J Neurooncol. 2005; 75:5–14. [PubMed: 16215811]

Gupta GP, Massagué J. Cancer metastasis: building a framework. Cell. 2006; 127:679–695. [PubMed: 17110329]

Gutierrez-Fernandez A, Gingles NA, Bai H, Castellino FJ, Parmer RJ, Miles LA. Plasminogen enhances neuritogenesis on laminin-1. J Neurosci. 2009; 29:12393–12400. [PubMed: 19812315]

Harbeck N, Thomssen C, Berger U, Ulm K, Kates RE, Hofler H, Janicke F, Graeff H, Schmitt M. Invasion marker PAI-1 remains a strong prognostic factor after long-term follow-up both for primary breast cancer and following first relapse. Breast Cancer Res Treat. 1999; 54:147–157. [PubMed: 10424405]

Heyn C, Ronald JA, Ramadan SS, Snir JA, Barry AM, MacKenzie LT, Mikulis DJ, Palmieri D, Bronder JL, Steeg PS, et al. In vivo MRI of cancer cell fate at the single-cell level in a mouse model of breast cancer metastasis to the brain. Magn Reson Med. 2006; 56:1001–1010. [PubMed: 17029229]

Irving JA, Pike RN, Lesk AM, Whisstock JC. Phylogeny of the serpin superfamily: implications of patterns of amino acid conservation for structure and function. Genome Res. 2000; 10:1845–1864. [PubMed: 11116082]

Kang Y, Siegel PM, Shu W, Drobnjak M, Kakonen SM, Cordón-Cardo C, Guise TA, Massagué J. A multigenic program mediating breast cancer metastasis to bone. Cancer Cell. 2003; 3:537–549. [PubMed: 12842083]

Karrison TG, Ferguson DJ, Meier P. Dormancy of mammary carcinoma after mastectomy. J Natl Cancer Inst. 1999; 91:80–85. [PubMed: 9890174]

Kienast Y, von Baumgarten L, Fuhrmann M, Klinkert WE, Goldbrunner R, Herms J, Winkler F. Real-time imaging reveals the single steps of brain metastasis formation. Nat Med. 2010; 16:116–122. [PubMed: 20023634]

Krammer PH. CD95's deadly mission in the immune system. Nature. 2000; 407:789–795. [PubMed: 11048730]

Kulahin N, Li S, Hinsby A, Kiselyov V, Berezin V, Bock E. Fibronectin type III (FN3) modules of the neuronal cell adhesion molecule L1 interact directly with the fibroblast growth factor (FGF) receptor. Mol Cell Neurosci. 2008; 37:528–536. [PubMed: 18222703]

Law RH, Zhang Q, McGowan S, Buckle AM, Silverman GA, Wong W, Rosado CJ, Langendorf CG, Pike RN, Bird PI, et al. An overview of the serpin superfamily. Genome Biol. 2006; 7:216. [PubMed: 16737556]

Leenders WP, Kusters B, Verrijp K, Maass C, Wesseling P, Heerschap A, Ruiter D, Ryan A, de Waal R. Antiangiogenic therapy of cerebral melanoma metastases results in sustained tumor progression via vessel co-option. Clin Cancer Res. 2004; 10:6222–6230. [PubMed: 15448011]

Li B, Wang C, Zhang Y, Zhao XY, Huang B, Wu PF, Li Q, Li H, Liu YS, Cao LY, et al. Elevated PLGF contributes to small-cell lung cancer brain metastasis. Oncogene. 2013; 32:2952–2962. [PubMed: 22797069]

Lin QBK, Fan D, Kim S-J, Guo L, Wang H, Bar-Eli M, Aldape KD, Fidler IJ. Reactive astrocytes protect melanoma cells from chemotherapy by sequestering intracellular calcium through gap junction communication channels. Neoplasia. 2010; 12:748–754. [PubMed: 20824051]

Lorger M, Felding-Habermann B. Capturing changes in the brain microenvironment during initial steps of breast cancer brain metastasis. Am J Pathol. 2010; 176:2958–2971. [PubMed: 20382702]

Maher EA, Mietz J, Arteaga CL, DePinho RA, Mohla S. Brain metastasis: opportunities in basic and translational research. Cancer Res. 2009; 69:6015–6020. [PubMed: 19638593]

Maness PF, Schachner M. Neural recognition molecules of the immunoglobulin superfamily: signaling transducers of axon guidance and neuronal migration. Nat Neurosci. 2007; 10:19–26. [PubMed: 17189949]

McMahon B, Kwaan HC. The plasminogen activator system and cancer. Pathophysiol Haemost Thromb. 2008; 36:184–194. [PubMed: 19176991]

Mechtersheimer S, Gutwein P, Agmon-Levin N, Stoeck A, Oleszewski M, Riedle S, Postina R, Fahrenholz F, Fogel M, Lemmon V, et al. Ectodomain shedding of L1 adhesion molecule promotes cell migration by autocrine binding to integrins. J Cell Biol. 2001; 155:661–673. [PubMed: 11706054]

Minn AJ, Gupta GP, Siegel PM, Bos PD, Shu W, Giri DD, Viale A, Olshen AB, Gerald WL, Massagué J. Genes that mediate breast cancer metastasis to lung. Nature. 2005; 436:518–524. [PubMed: 16049480]

Muller WJ, Sinn E, Pattengale PK, Wallace R, Leder P. Single-step induction of mammary adenocarcinoma in transgenic mice bearing the activated c-neu oncogene. Cell. 1988; 54:105–115. [PubMed: 2898299]

Nayeem N, Silletti S, Yang X, Lemmon VP, Reisfeld RA, Stallcup WB, Montgomery AM. A potential role for the plasmin(ogen) system in the posttranslational cleavage of the neural cell adhesion molecule L1. J Cell Sci. 1999; 112(Pt 24):4739–4749. [PubMed: 10574721]

Nguyen DX, Chiang AC, Zhang XH, Kim JY, Kris MG, Ladanyi M, Gerald WL, Massagué J. WNT/TCF signaling through LEF1 and HOXB9 mediates lung adenocarcinoma metastasis. Cell. 2009; 138:51–62. [PubMed: 19576624]

Pang PT, Teng HK, Zaitsev E, Woo NT, Sakata K, Zhen S, Teng KK, Yung WH, Hempstead BL, Lu B. Cleavage of proBDNF by tPA/plasmin is essential for long-term hippocampal plasticity. Science. 2004; 306:487–491. [PubMed: 15486301]

Polleux F, Ghosh A. The slice overlay assay: a versatile tool to study the influence of extracellular signals on neuronal development. Sci STKE. 2002; 136:19–29.

Schafer MK, Altevogt P. L1CAM malfunction in the nervous system and human carcinomas. Cell Mol Life Sci. 2010; 67:2425–2437. [PubMed: 20237819]

Schroder C, Schumacher U, Fogel M, Feuerhake F, Muller V, Wirtz RM, Altevogt P, Krenkel S, Janicke F, Milde-Langosch K. Expression and prognostic value of L1-CAM in breast cancer. Oncol Rep. 2009; 22:1109–1117. [PubMed: 19787228]

Seike T, Fujita K, Yamakawa Y, Kido MA, Takiguchi S, Teramoto N, Iguchi H, Noda M. Interaction between lung cancer cells and astrocytes via specific inflammatory cytokines in the microenvironment of brain metastasis. Clin Exp Metastasis. 2011; 28:13–25. [PubMed: 20953899]

Silletti S, Mei F, Sheppard D, Montgomery AM. Plasmin-sensitive dibasic sequences in the third fibronectin-like domain of L1-cell adhesion molecule (CAM) facilitate homomultimerization and concomitant integrin recruitment. J Cell Biol. 2000; 149:1485–1502. [PubMed: 10871287]

Sofroniew MV, Vinters HV. Astrocytes: biology and pathology. Acta Neuropathol Suppl (Berl). 2010; 119:7–35.

Takehara S, Onda M, Zhang J, Nishiyama M, Yang X, Mikami B, Lomas DA. The 2.1-A crystal structure of native neuroserpin reveals unique structural elements that contribute to conformational instability. J Mol Biol. 2009; 388:11–20. [PubMed: 19285087]

Teesalu T, Hinkkanen AE, Vaheri A. Coordinated induction of extracellular proteolysis systems during experimental autoimmune encephalomyelitis in mice. Am J Pathol. 2001; 159:2227–2237. [PubMed: 11733372]

Valastyan S, Weinberg RA. Tumor metastasis: molecular insights and evolving paradigms. Cell. 2011; 147:275–292. [PubMed: 22000009]

Vanharanta S, Massague J. Origins of metastatic traits. Cancer Cell. 2013; 24:410–421. [PubMed: 24135279]

Vos YJ, Hofstra RM. An updated and upgraded L1CAM mutation database. Hum Mutat. 2010; 31:E1102–E1109. [PubMed: 19953645]

Voura EB, Ramjeesingh RA, Montgomery AM, Siu CH. Involvement of integrin alpha(v)beta(3) and cell adhesion molecule L1 in transendothelial migration of melanoma cells. Mol Biol Cell. 2001; 12:2699–2710. [PubMed: 11553709]

Wang X, Haroon F, Karray S, Martina D, Schluter D. Astrocytic Fas ligand expression is required to induce T-cell apoptosis and recovery from experimental autoimmune encephalomyelitis. Eur J Immunol. 2013; 43:115–124. [PubMed: 23011975]

Wiencken-Barger AE, Mavity-Hudson J, Bartsch U, Schachner M, Casagrande VA. The role of L1 in axon pathfinding and fasciculation. Cereb Cortex. 2004; 14:121–131. [PubMed: 14704209]

Winslow MM, Dayton TL, Verhaak RG, Kim-Kiselak C, Snyder EL, Feldser DM, Hubbard DD, DuPage MJ, Whittaker CA, Hoersch S, et al. Suppression of lung adenocarcinoma progression by Nkx2-1. Nature. 2011; 473:101–104. [PubMed: 21471965]

Yepes M, Sandkvist M, Wong MK, Coleman TA, Smith E, Cohan SL, Lawrence DA. Neuroserpin reduces cerebral infarct volume and protects neurons from ischemia-induced apoptosis. Blood. 2000; 96:569–576. [PubMed: 10887120]

Highlights

- Metastatic cells in the brain survive and grow attached to capillaries
- Plasmin from the reactive stroma mobilizes FasL to repel brain-infiltrating cells
- Plasmin additionally prevents vascular cooption by cleaving cancer cell L1CAM
- Brain metastatic cells express Serpins to avoid Plasmin production

A

Cell line	Species	Tumor type	Source	Serpin mRNA (relative level)			
				I1 (NS)	*B2*	*E2*	*D1*
H2030-BrM3	Human	Lung adenocarcinoma (*KRAS* mutant)	Lymph node	3.4	0.3	1.4	0.3
PC9-BrM3	Human	Lung adenocarcinoma (*EGFR* mutant)	Lymph node	1.2	0.7	0.8	2.8
MDA231-BrM2	Human	TN breast carcinoma (ER-, PR-, HER2-)	Pleural fluid	5.0	10.1	0.5	5.1
CN34-BrM2	Human	TN breast carcinoma (ER-, PR-, HER2-)	Pleural fluid	8.9	15.5	9.6	8.5
Kras/p53-482N1	Mouse	Lung adenocarcinoma (*Kras* mutant, *p53* null)	Lymph node	4.3	2.9	37.6	62.2
ErbB2-BrM2	Mouse	Breast carcinoma (*ErbB2* hyperactive)	Mammary tumor	0.5	15.7	1.9	7.0

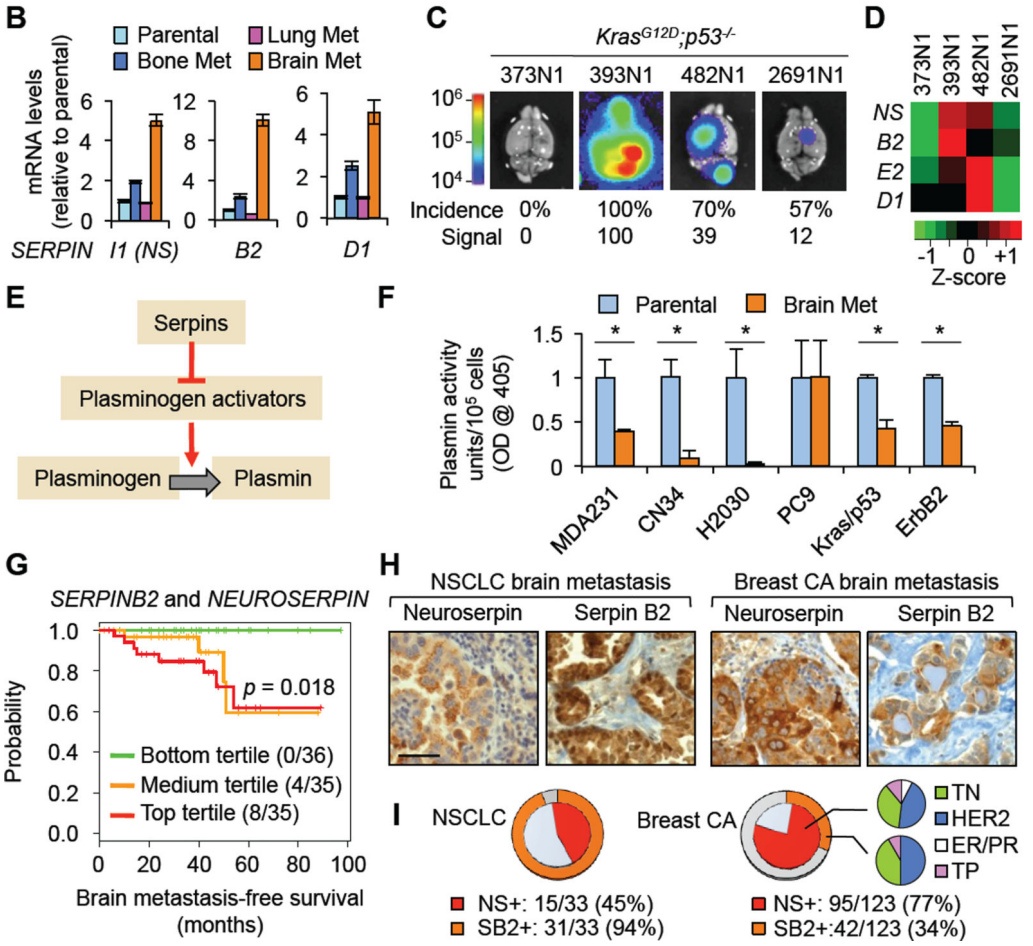

Figure 1. Association of PA-inhibitory serpins with the brain metastatic phenotype

(A) Serpin mRNA levels in brain metastatic cell lines relative to the levels in counterparts not metastatic to brain. TN, triple negative; ER−, estrogen receptor negative, PR−, progesterone receptor negative. (B) mRNA levels of the indicated serpins in the parental MDA231 cell line and derivatives with different metastatic tropisms. Error bars, 95% confidence interval. (C) Representative ex vivo bioluminescence (BLI) images of brains from syngeneic mice inoculated with *Kras*^{G12D};*p53*$^{-/-}$ mouse lung cancer cell lines. The percentage of mice developing brain metastasis and the mean BLI photon flux signal are

indicated. n=10 (D) Heatmap of serpin mRNA expression in *Kras*^{G12D};*p53*$^{-/-}$ derivatives. (E) Summary of the serpin-PA-plasmin cascade. (F) Inhibition of plasminogen conversion into plasmin by cell culture supernatants of the indicated cell lines. Plasmin activity was determined by a chromogenic assay. Data are averages ± SEM from triplicate experiments. (G) Kaplan-Meier analysis of brain metastasis-free survival in 106 cases of lung adenocarcinoma classified based on *SERPINB2* and *SERPINI1* mRNA levels in the primary tumor. P value calculated from a Cox proportional hazard model, with *SERPINB2* and *SERPINI1* expression treated as a continuous variable. (H) Representative human brain metastasis samples from lung and breast cancer stained with antibodies against NS or serpin B2. (I) Proportion of metastasis samples scoring positive for NS immunostaining (red) or serpin B2 immunostaining (orange) in 33 cases of non-small cell lung carcinoma and 123 cases of breast carcinoma. Small diagrams in the breast cancer set represent the primary tumor subtype (HER2, HER2+; ER/PR, hormone-receptor positive; TP, triple positive) of the serpin-positive samples for which this information was available. Brain metastases scoring positive for both serpins comprise 42% and 34% of the lung cancer and breast cancer cases, respectively. Samples scored as positive had >80% of neoplastic cells showing positive reactivity. Scale bar: 100μm.

See also Figure S1.

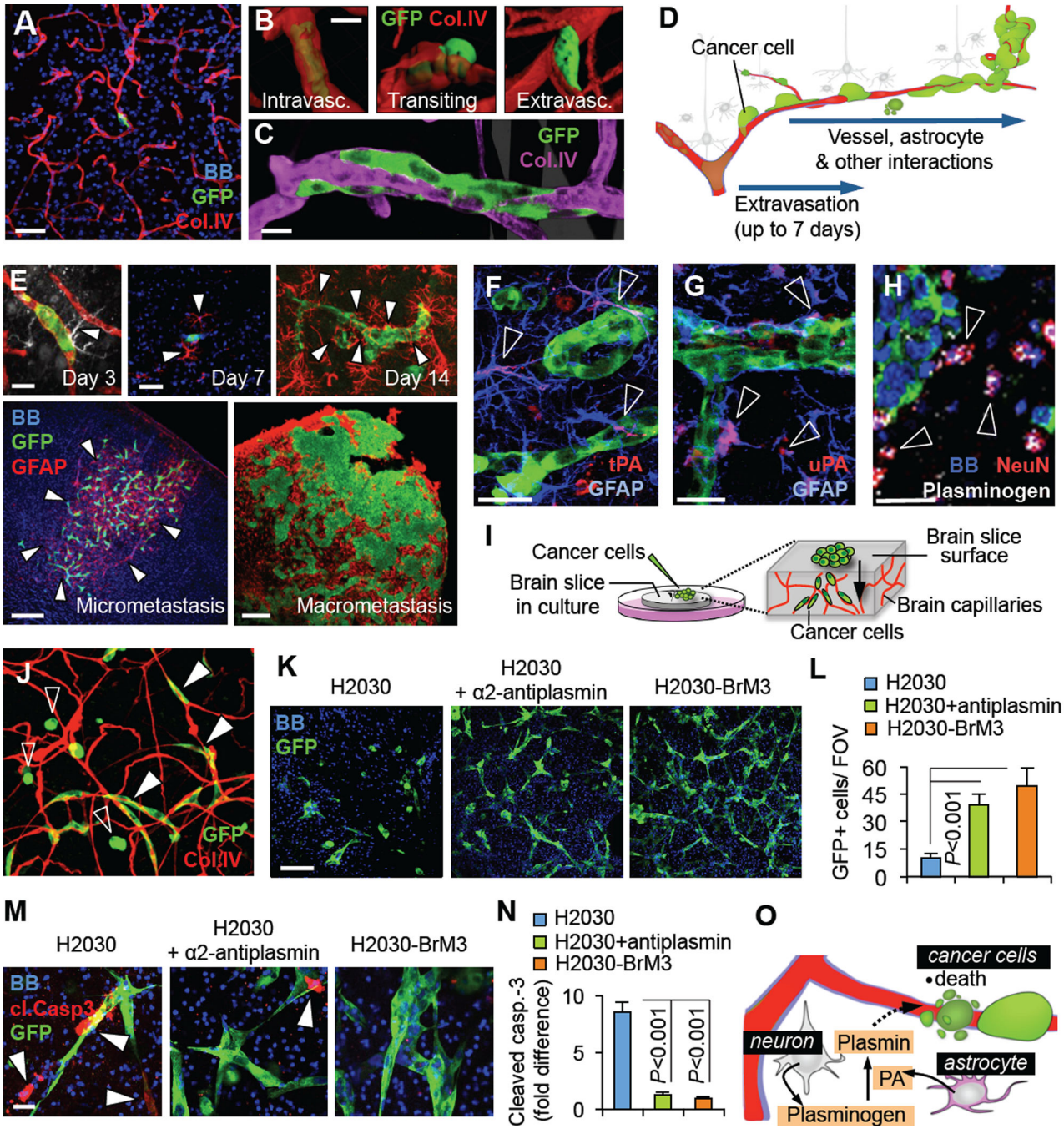

Figure 2. Vascular cooption, outgrowth, and escape from stromal plasmin action

(A) Metastatic cell interactions with brain capillaries. MDA231-BrM2 cells (green) remain bound to brain capillaries (red) after completing extravasation. (B) Confocal analysis of the extravasation steps showing a GFP+ MDA231-BrM2 cell. (C) Cluster of extravasated MDA231-BrM2 cells forming a furrow around a brain capillary. All extravasated cells initially grew in this manner. Blue, nuclear staining. (D) Schema representing the initial steps and interactions during metastatic colonization of the brain. (E) Exposure of metastatic H2030-BrM3 cells to GFAP+ reactive astrocytes (arrowheads) in the brain parenchyma at

different time points after inoculation of cancer cells into the circulation. Day 3: red, collagen IV; white, GFAP; green, GFP+ cancer cells. Blue, nuclear staining. (F,G) tPA and uPA immunofluorescence staining (arrowheads) associated with GFAP+ astrocytes in a mouse brain harboring GFP+ H2030-BrM3 cells (green). (H) Plasminogen immunofluorescence staining (white, arrowheads) is associated with NeuN+ neuron bodies (red) near a cluster of GFP+ metastatic cells (green) in a mouse brain. Blue, nuclei. (I) Schema of brain slice organotypic cultures. Cancer cells placed on the surface of slices migrate into the tissue and seek microcapillaries. (J) Representative image of a brain slice harboring infiltrated H2030-BrM3 cells that are still round (open arrowheads) or already spread over brain capillaries (closed arrowheads). (K) Representative confocal images of brain slice tissue infiltrated with the indicated cancer cells. α2-antiplasmin was added to the indicated cultures. Note the lower density and disorganized aspect of parental cells compared with the stretched morphology of BrM3 cells or parental cells with α2-antiplasmin. (L) Quantification of GFP+ cancer cells in the experiments of panel K. Number of cells per field of view (FOV) are averages ± SEM. n=6–10 brain slices, scoring at least two fields per slice, in at least 2 independent experiments. (M) Cleaved caspase-3 immunofluorescence staining in brain slices harboring the indicated cells and additions. (N) Quantification of cleaved caspase-3 positive cancer cells in the experiments of panel M. Values are quantified as panel L, normalized to H2030-BrM3, and are averages ± SEM. (O) Schematic summary showing neurons and astrocytes as sources of plasminogen and PA, respectively, and lethal effect of the resulting plasmin on infiltrating cancer cells. All P values by Student’s t-test. Scale bars: 25μm (A), 5μm (B–C), 5μm (Day 3), 15μm (Day 7), 25μm (Day 14), 70μm (micrometastasis), 100μm (macrometastasis) (D), 10μm (F–H), 100μm (K), 5μm (M)

See also Figure S2.

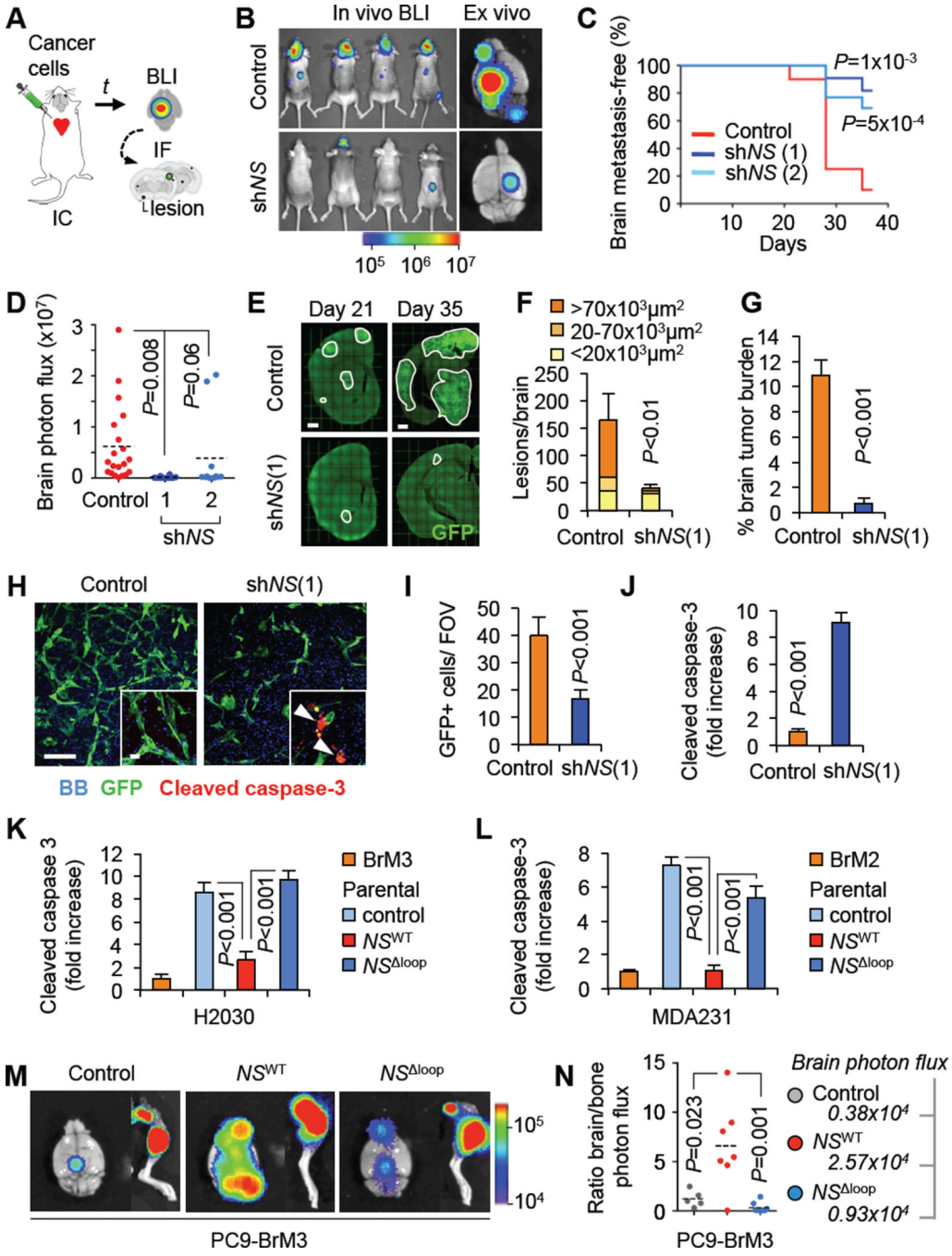

Figure 3. Neuroserpin mediates brain metastasis

(A) Schema of experimental design. (B) Representative images of whole-body BLI and brain ex vivo BLI 5 weeks after inoculation of H2030-BrM3 cells transduced with control shRNA or *NS* shRNA (sh*NS*). (C) Kaplan–Meier plot of brain metastasis-free survival in the experiment of panel B. Control (n=20) and two different sh*NS* [sh*NS* (1), n=11; sh*NS* (2), n=13] were analyzed. P values were obtained with log rank Mantel-Cox test. (D) Quantification of ex vivo BLI in brains from panel B. (E) Representative images of coronal brain sections analyzed for GFP IF 21 or 35 days after inoculation of H2030- BrM3 cells

into mice. Lesion contours are marked. (F) Quantification of brain lesions according to size at 21 day time point in panel E. Control n=5, sh*NS* n=6 brains. P value refers to size distribution. For the total number of lesions, $p<0.05$. (G) Quantification of brain tumor burden in the experiment of panel E. Control n=5, sh*NS* n=6. (H) Representative images of control and *NS*-depleted H2030-BrM3 cells in brain slice assays. Insets show cleaved caspase-3 IF. (I,J) Quantification of GFP+ cells (I) and cleaved caspase-3 (J) in the experiment of panel H. Data are averages ± SEM. n=6–10 slices, scoring at least two fields per slice, in at least 2 independent experiments. (K,L) Quantification of cells that were positive for cleaved caspase-3 comparing parental and BrM cell lines, and the effect of overexpressing NS wild type (NS^{WT}) or a mutant form unable to target PA ($NS^{\Delta loop}$) in parental cell lines H2030 (K) and MDA231 (L). Data are averages ± SEM, quantified as panel J. (M) Representative ex vivo BLI images of brains and hindlimbs from mice 21 days after inoculation with PC9-BrM3. Cells were transduced with empty vector (n=5) or NS^{WT} (n=7) or $NS^{\Delta loop}$ mutant (n=8). (N) Ratio of photon flux in brain versus bone in the experiment of panel M. Ex vivo brain mean BLI values are also shown. All P values were calculated by Student's t-test, except in panel C. Scale bar: 250μm (E), 100μm, 5μm (inset) (H).

See also Figure S3.

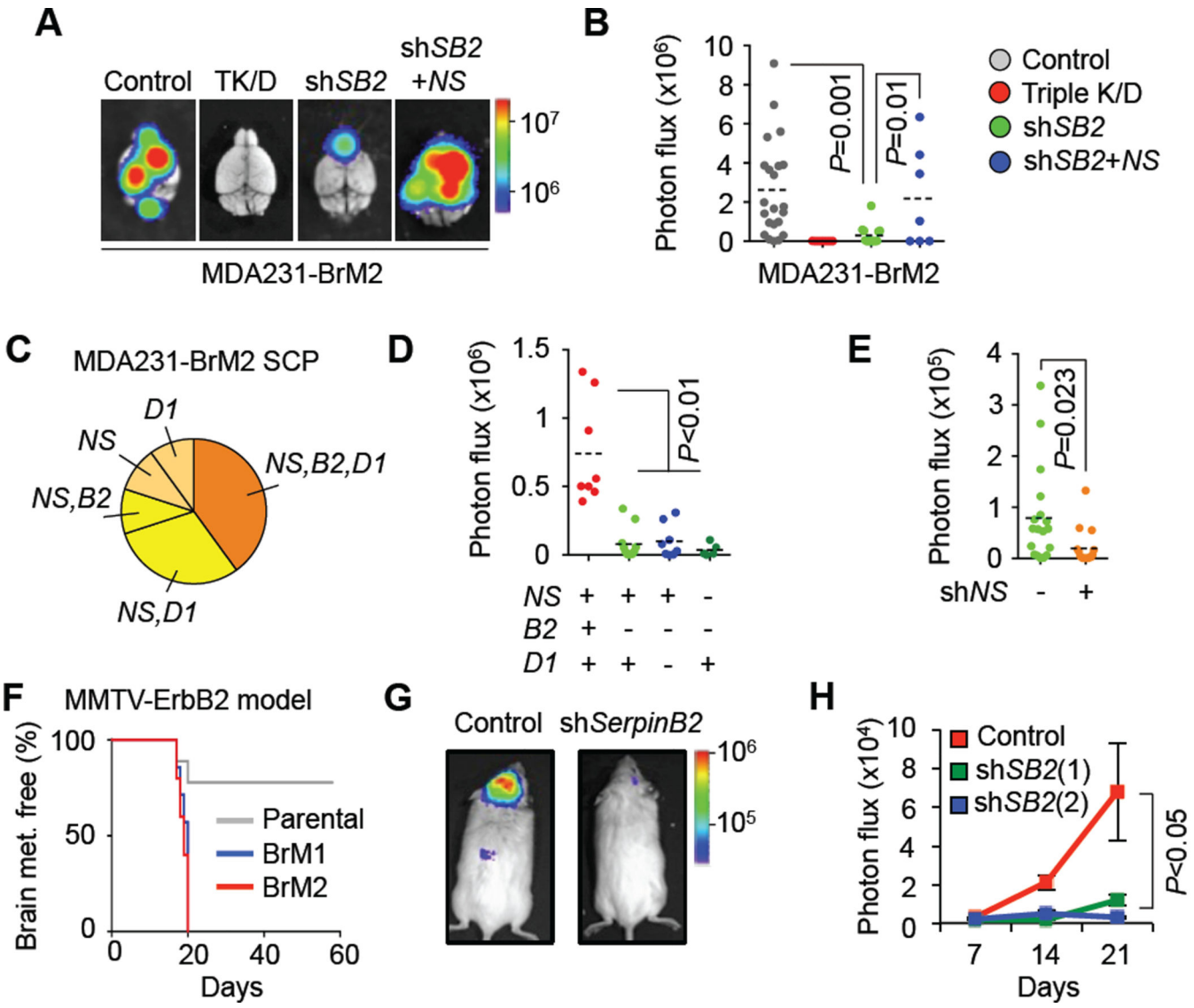

Figure 4. Anti-PA serpins mediate brain metastasis by breast cancer cells

(A,B) MDA231-BrM2 cells transduced with control vector, shRNA vectors targeting *NS*, *SERPINB2* and *SERPIND1* (triple K/D), *SERPINB2* shRNA (sh*SB2*), or sh*SB2* plus a NS expressing vector were inoculated into the arterial circulation of immunodeficient mice. Brain metastasis burden was visualized by ex vivo brain BLI (A) and quantitated (B). Control n=22; triple K/D n=9, sh*SB2* n=14; sh*SB2* and NS n=8. (C) Distribution of clones (single cell progenies –SCP−) overexpressing one, two, or three of the indicated serpins among ten clonal cell lines isolated from the MDA231-BrM2 population. (D) Ex vivo brain BLI quantification from different MDA231-BrM2 SCP injected. Red dots SCP (high levels of all serpins), n=8; light green dots SCP (low levels of serpin B2), n=11; blue dots SCP (low levels of serpin B2 and D1), n=8; dark green dots SCP (low levels of serpin B2 and NS), n=5. P value was determined by Student's t-test. (E) SCP with high levels of NS and serpin D1 were subjected to *NS* knockdown and tested for brain metastatic activity. (F) Kaplan–Meier survival curves for brain metastasis-free survival in syngeneic mice

inoculated with parental ErbB2-P cells (n=9) or brain metastatic derivatives ErbB2-BrM1 (n=7) and ErbB2-BrM2 (n=5). Survival curves were compared using log rank Mantel-Cox test. ErbB2-P versus ErbB2-BrM1, *P*=0.0045, and versus ErbB2-BrM2 *P*=0.0053. (G,H) Representative images (G) and quantification (H) of brain metastasis BLI photon flux formed by ErbB2-BrM2 or these cells expressing two different serpin *B2* shRNAs (sh*SB2*). Control, n=10; sh*SB2* (1), n=10; sh*SB2* (2), n=6. Data are averages ± SEM. All P values were determined by Student's t-test, except in panel G.
See also Figure S4.

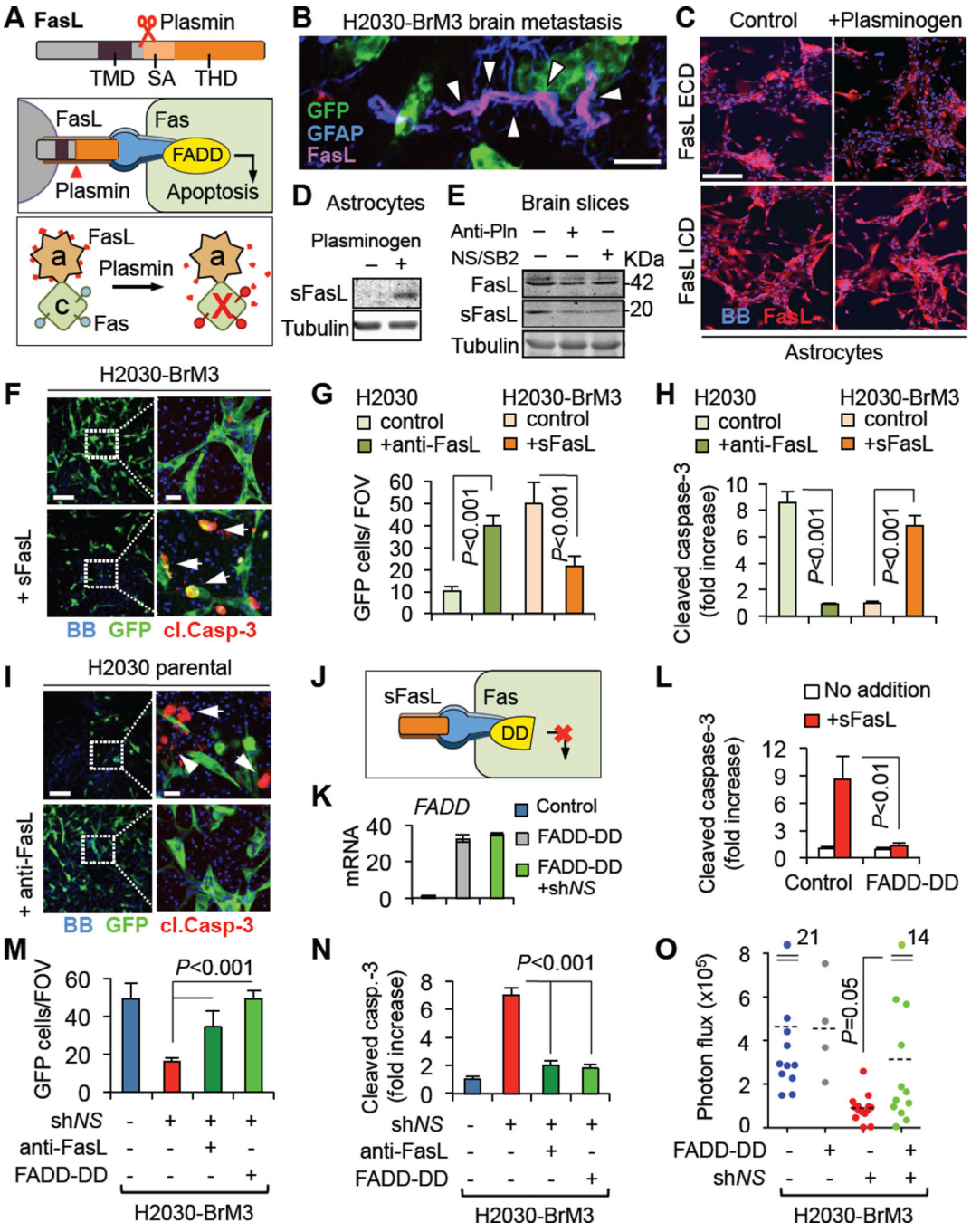

Figure 5. Neuroserpin shields cancer cells from FasL death signals

(A) Schema of FasL and its conversion by plasmin into sFasL, a diffusible trigger of apoptosis through Fas-FADD signaling. TMD, transmembrane domain; SA, trimeric self-assembly domain; THD, tumor necrosis factor-homology domain. Red crosses, apoptotic cells. a, astrocyte. c, cancer cell. (B) IF with antibodies against GFP (cancer cells), GFAP (reactive astrocytes) and FasL in a mouse brain harboring metastatic cells 21 days after arterial inoculation of H2030-BrM3. (C) Images of astrocyte cultures incubated with exogenous plasminogen (1μM) or no additions. Staining was performed with antibodies

against the extracellular domain (ECD) or the intracellular domain of FasL (ICD). (D) Western immunoblotting of supernatants from cultures shown in panel C, using anti-FasL ECD antibodies. (E) Mouse brain slices were incubated with α2-antiplasmin, NS and serpin B2, or no additions. sFasL in tissue lysates was detected by western immunoblotting with anti-FasL ECD. Quantification of band density relative to tubulin (left to right) yielded sFasL:FasL ratios of 1, 0.51, 0.28. (F) GFP+ H2030-BrM3 cells (green) were allowed to infiltrate brain slices in media containing added sFasL or no additions and scored for cleaved caspase-3 (red, in inset). (G, H) Quantification of total GFP+ cells (G), and apoptotic GFP+ cells (H) in the experiments of panels F (orange bars) and I (green bars). Data are averages ± SEM. n=6–10 slices, scoring at least two fields per slice, from at least 2 independent experiments. (I) GFP+ H2030 cells (green) were allowed to infiltrate brain slices in media containing anti-FasL blocking antibody or no additions. Anti-FasL prevented endogenous signals from triggering caspase-3 activation (red, in inset). (J) Depiction of FADD-DD overexpression (yellow shape) to suppress pro-apoptotic Fas signaling in cancer cells. (K) *FADD* expression in H2030-BrM3 transduced with a FADD-DD vector. (L) Quantification of apoptotic cells following sFasL addition to H2030-BrM3 cells transduced with the indicated vectors. (M, N) Quantification of total GFP+ cells (M), and apoptotic GFP+ cells (N) in brain slices harboring the indicated GFP+ H2030-BrM3 transfectants and/or additions. Data are averages ± SEM, and quantitated as panels G,H. (O) Brain metastatic activity of H2030-BrM3 cells transduced with the indicated vectors and inoculated into the arterial circulation of mice. BLI photon flux was quantitated in cells transduced with control shRNA (n=11), FADD-DD (n=4), *NS* shRNA (n=14), or this shRNA and FADD-DD (n=12). All P values were determined by Student's t-test. Scale bars: 25μm (B), 200μm (C), 100μm (F,I), 5μm (insets in F,I).
See also Figure S5.

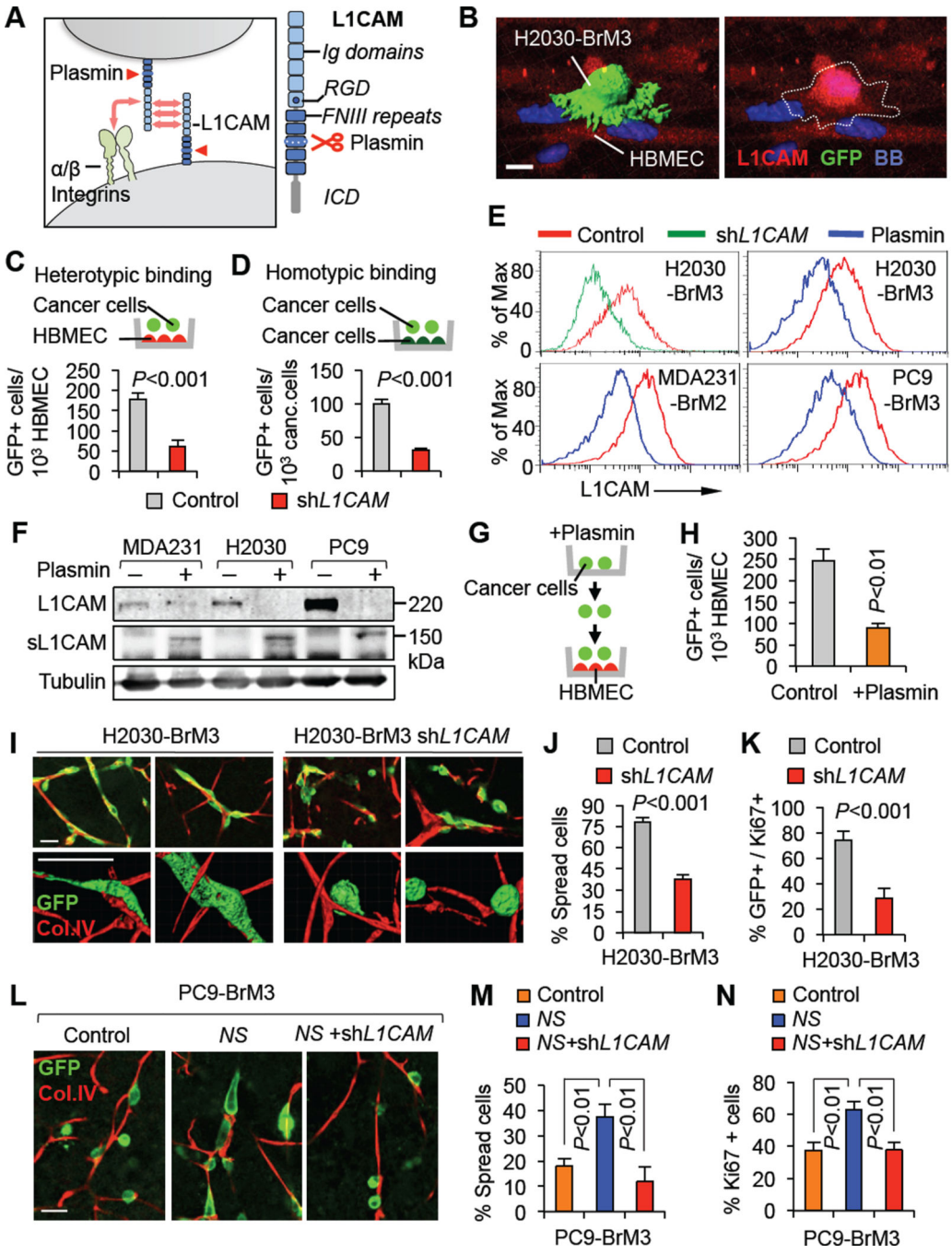

Figure 6. The plasmin target L1CAM mediates vascular cooption by brain metastatic cells

(A) Schema of L1CAM as a mediator of homophilic and heterophilic (e.g., integrins) cell adhesive interactions, and its conversion by plasmin into an adhesion defective fragment. Immunoglobulin-like (Ig) and fibronectin type III (FNIII) domain repeats, the intracellular domain (ICD), and an integrin-binding RGD sequence are indicated. (B) Suspensions of GFP+ H2030-BrM3 cells were placed on top of a monolayer of human brain microvascular endothelial cells (HBMEC) (C, D) Analysis of H2030-BrM3 binding to HBMEC monolayers (C) or to H2030-BrM3 monolayers (D), and effect of L1CAM knockdown. Data

are averages ± SEM. n=5, scoring at least 10 fields per coverslip. (E) Flow cytometry of cell-surface L1CAM in the indicated brain cells expressing *L1CAM* shRNA or incubated with plasmin, compared to untreated controls. (F) Anti-L1CAM western immunoblotting of cells and culture supernatants after incubation with or without plasmin. (G,H) Cancer cells were treated with plasmin and subjected to HBMEC adhesion assays. Data are averages ± SEM. n=3, scoring at least 5 fields per coverslip. (I) Control or *L1CAM*-depleted H2030-BrM3 cells after infiltrating brain tissue slices. GFP+ cancer cells (green) and vasculature (collagen IV immunostaining, red) were visualized after 2 days. Two representative images are shown per condition. Lower panels, high magnification. (J,K) Quantification of cells that were spread on capillaries (J) and Ki67+ cells (K) in the experiments of panel I. Data are averages ± SEM. n=6 slices, scoring at least three fields per slice, from 2 independent experiments. (L) Effect of NS overexpression and *L1CAM* depletion on the interaction of PC9-BrM3 cells with capillaries in brain slices. (M,N) Quantification of cells that were spread on capillaries (M) and Ki67+ cells (N) in the experiments of panel L. Data are averages ± SEM, and quantitated as panels J,K. All P values by Student's t-test. Scale bars: 10μm (B), 50μm (I,L).

See also Figure S6.

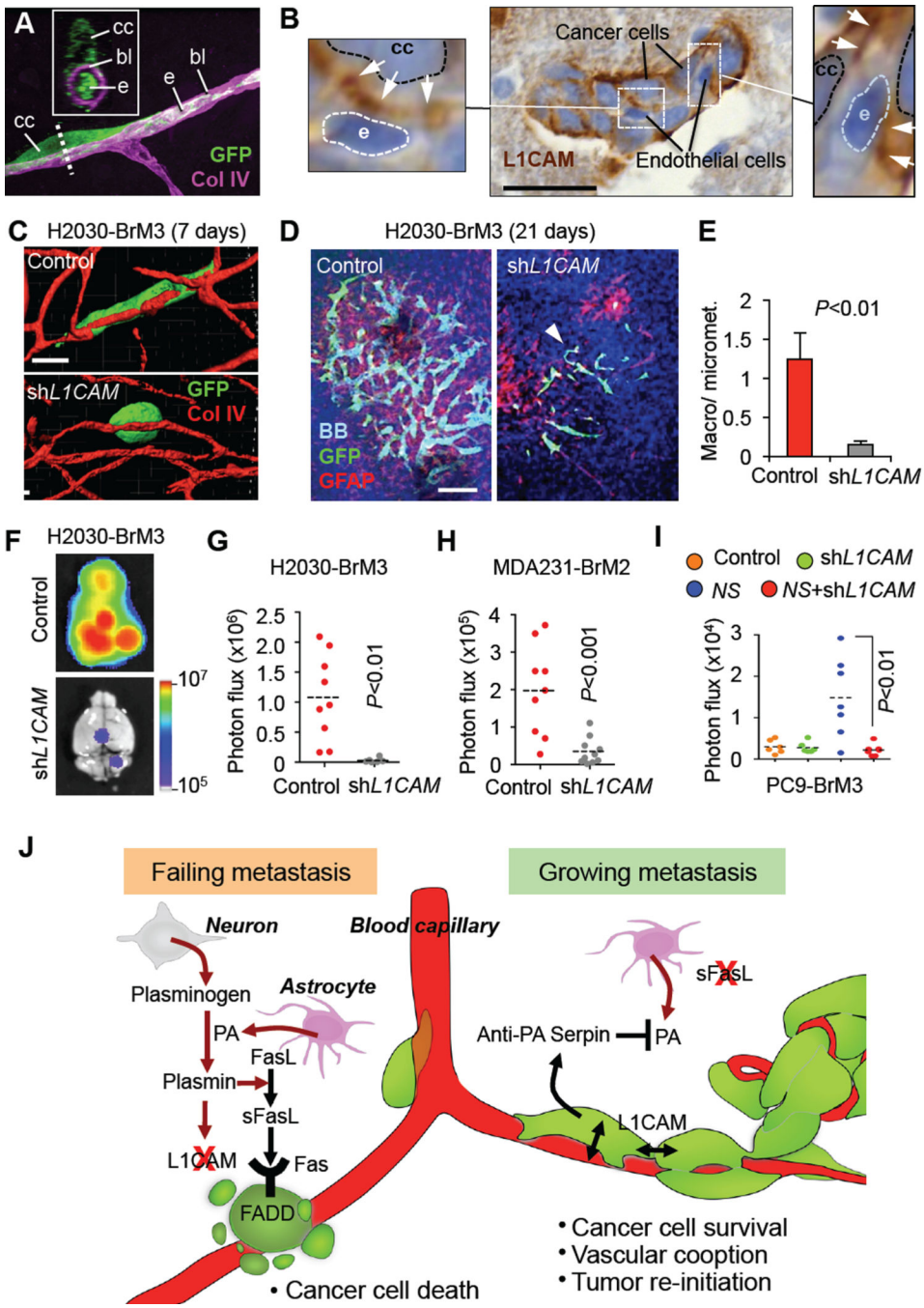

Figure 7. L1CAM mediates metastatic outgrowth in the brain

(A) GFP+ H2030-BrM3 co-opting the basal lamina rich in collagen IV of endothelial cells labeled with VE-cadherin in brain slices. bl, basal lamina; e, endothelium; cc, cancer cell. (B) Immunohistochemical staining with anti-L1CAM antibodies and H&E counterstaining of incipient brain colonies formed by H2030-BrM3. Cancer cells (cc, pale blue nuclei) remain close to each other and interact with endothelial cells (e, dark blue nuclei). Insets, higher magnification of cell-cell contact areas. (C) H2030-BrM3 cells infiltrating the brain 7 days after intracardiac injection, and effect of *L1CAM* depletion. (D) Representative images

of GFP+ metastatic lesions from brains in panel C. (E) Relative abundance of macrometastasis over micrometastasis (as defined in Figure 3F) in brains shown in panel D. Number of lesions: control= 283.2 ± 84.8, sh*L1CAM*= 69.8 ± 11.5. Data are averages ± SEM. n=3 brains. (F,G) Representative images (F) and quantification (G) of ex vivo brain BLI from mice inoculated with indicated H2030-BrM3 cells. Control shRNA, n=9; sh*L1CAM*, n=6. (H) Quantification of ex vivo brain BLI from mice that were arterially inoculated with indicated MDA231-BrM2 cells. Control shRNA, n=9; sh*L1CAM*, n=10. (I) Quantification of ex vivo brain BLI from mice that were arterially inoculated with the indicated PC9-BrM3 cells (n=5–7). All P values were determined by Student's t-test. Scale bar: 25μm (B), 30μm (F), 200μm (G). (J) Model of the action of the stromal PA-plasmin system against cancer cells that infiltrate the brain, and role of anti-PA serpins in protecting brain metastatic cells from stromal PA-plasmin. Reactive astrocytes produce PAs in the presence of extravasated cancer cells. Metastasis fails (left side) when PAs generate plasmin from neuron-derived plasminogen and plasmin mobilizes FasL from astrocytes to kill cancer cells. Additionally, plasmin cleaves and inactivates L1CAM, a cell adhesion molecule that cancer cells express for vascular cooption. Metastasis proceeds (right side) when brain metastatic cells express anti-PA serpins that prevent the generation of plasmin and its deleterious effects on the survival and vascular attachment of the cancer cells.
See also Figure S7.